

PACS numbers: 42.65.Ky; 42.60.Da; 42.60.Lh
DOI: 10.1070/QE2005v035n09ABEH003440

Intracavity frequency doubling in a wide-aperture argon laser

S.R. Abdullina, S.A. Babin, A.A. Vlasov, S.I. Kablukov

***Abstract*. The four-mirror cavity with a BBO crystal for frequency doubling in a wide-aperture argon laser is optimised. The dependences of the second-harmonic power on the displacement of a focusing mirror, the displacement of the crystal, and the discharge current are measured. These dependences are in good agreement with calculations. After optimisation, ~ 1 W of UV laser radiation at 244 nm was obtained with the conversion efficiency twice as large as that for the known similar lasers. It is shown that the increase in the efficiency was achieved mainly due to the increase in the discharge-tube aperture.**

Keywords: *argon laser, intracavity frequency doubling, ultraviolet radiation.*

1. Introduction

The writing of Bragg gratings in an optical fibre is of great interest for optical communication systems and sensors. This process requires high-power ($P \geqslant 50$ mW), short-wavelength radiation ($\lambda < 250$ nm) with the large coherence length ($l_c \geqslant 1$ cm) [1]. A radiation beam with such properties can be obtained after the intracavity frequency doubling in an argon laser or doubling of single-frequency radiation in an external cavity. In the case of intracavity doubling, the output radiation power can be much higher than upon frequency doubling in an external cavity; however, the coherence length of radiation is considerably smaller (1 – 5 cm compared to 1 – 10 m).

The intracavity frequency doubling in a capillary (the discharge-channel diameter is $D \leqslant 2.5$ mm) argon laser ($\lambda = 514.5$ nm) was first performed in ADP and KDP crystals in 1968 [2]. The doubling conversion efficiency η was 2×10^{-3} W^{-1}, and the maximum power of the second harmonic was 415 mW. The highest output second-harmonic power was achieved in 1992 [3]. The cw power at 257 nm was 1.2 W after the intracavity frequency doubling of radiation from an argon laser in a BBO crystal.

The frequency doubling of a single-frequency 514.5-nm laser beam of an elliptic cross section in a BBO crystal placed in an external ring resonator was performed in 1995 [4]. The output second-harmonic power achieved 500 mW for the input power equal to 2 W. Note that during frequency doubling in an external resonator, the laser frequency should be matched with the resonator frequency. This was provided by using the polarisation method for automatic frequency control [5]. In 1997, 2 W of second-harmonic power was obtained by doubling the 5.6-W, 514.5-nm line frequency in a BBO crystal in an external resonator [6].

The most powerful commercial argon laser is a Coherent Innova Sabre Fred laser with the intracavity frequency doubling in a BBO crystal. The emission wavelength of this laser can be tuned in the spectral range from 229 to 264 nm. The maximum output power of the laser at 514.5 nm is 8 W and at the second harmonic (at 257 nm) – 1 W, i.e., the conditional conversion efficiency is 12.5 %. The output power at the 488-nm line is 6.5 W, while the second-harmonic power at 244 nm is 0.5 W, i.e., the conversion efficiency for the 488-nm line is considerably lower than that for the 514-nm line, being only ~ 8 %.

Among commercial systems for frequency doubling in an external resonator, a Spectra Physics Wave Train CW Frequency Doubler can be pointed out. Doubling is performed in the 410 – 500-nm range in a BBO crystal, the conversion efficiency is 4 % – 8 %, and the second-harmonic power at 255 nm is ~ 100 mW (see also [7]).

The aim of this paper is to increase the second-harmonic power at 244 nm upon intracavity frequency doubling. For this purpose, we used a wide-aperture ($D = 6$ mm) argon laser with a BBO crystal and optimised the parameters of a four-mirror cavity.

2. Calculation of a four-mirror cavity

We studied a four-mirror cavity shown schematically in Fig. 1. To increase the radiation power in the visible range, we used a tube of a larger diameter, which provided the high efficiency with respect to power supplied to the discharge tube and allowed an increase in the diameter of the fundamental-mode beam in the four-mirror scheme [8]. In this scheme in the case of incomplete filling of the active medium by laser radiation, the focusing arm of the cavity can be adjusted in a broader range than in the scheme with a capillary tube. This permits additional optimisation of the frequency-doubling regime. In this case, the cavity of optimal configuration should have a large cross section of the beam in the $R_1 - R_{11}$ arm to provide the efficient use of the active medium and ensure a sufficiently tight focusing of radiation in the crystal for efficient frequency doubling.

S.R. Abdullina, S.A. Babin, A.A. Vlasov, S.I. Kablukov Institute of Automation and Electrometry, Siberian Branch, Russian Academy of Sciences, prop. akad. Koptyuga 1, 630090 Novosibirsk, Russia; e-mail: kab@iae.nsk.su

Received 19 November 2004; revision received 17 June 2005
Kvantovaya Elektronika **35** (9) 857 – 861 (2005)
Translated by M.N. Sapozhnikov

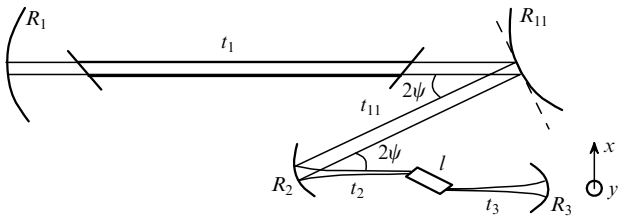

Figure 1. Scheme of the four-mirror cavity: R_i: mirrors with the corresponding radii of curvature; t_i: arm lengths; l: crystal length; 2ψ: angle of bending.

It is known that focusing is optimal when the confocal parameter of the beam $b = 2\pi n_0 w^2/\lambda$ is approximately equal to the crystal length (where w is the caustic radius and n_0 is the refractive index). For our crystal of length $l = 10$ mm for $\lambda = 488$ nm, the waist with $w \sim 20\mu$m corresponds to such a confocal parameter.

We used a BBO crystal with the type ooe phase matching. For the wavelength 488 nm, the phase-matching angle is $\theta_s = 54.5^\circ$, the Brewster angle is $\theta_B = 59.2^\circ$, and the walk-off angle is $\rho = 83$ mrad [9]. The temperature phase-matching width for this crystal is 4.6 °C cm and the angular phase-matching width is 0.18 mrad cm.

We performed calculations for six configurations of the four-mirror cavity differing in the radii of curvature R_1 and R_{11} of mirrors: configurations 1 ($R_1 = 10$ m, $R_{11} = \infty$), 2 (10 m, −10 m), 3 (−10 m, 10 m), 4 (∞, 10 m), 5 (∞, −10 m) and 6 (∞, ∞). The following parameters remained constant for all configurations of the cavity: $R_2 = 12.8$ cm, $R_3 = 6.0$ cm, $l = 1$ cm, $t_1 = 1.86$ m, $t_{11} = 0.14$ m, $t_2 = \frac{1}{2}t_0 + \delta t$ and $t_3 = \frac{1}{2}t_0 - \delta t$, where $\delta t \sim 1 - 2$ mm characterises the displacement of the crystal with respect to the middle of the $R_2 - R_3$ arm and for the specified variable parameter t_0 determines the position of beam waists in the crystal.

2.1 Calculation method

The calculation was performed by the ABCD matrix method of transformation of Gaussian beams separately for the tangential (x) and sagittal (y) planes. Matrix elements were taken from handbook [10].

Consider the calculation scheme for configuration 1 of the cavity. By using the parameters presented above, we calculated the beam parameters at an arbitrary site of the cavity, in particular, on the mirror R_{11} and constructed plots of the dependence of the beam radius on these mirrors on the distance t_0, from which we determined the optimal angle of incidence on the mirror R_2 and stability regions of the cavity in both planes. For configuration 1, the optimal angle of incidence was $\psi = 13.8^\circ$. In this case, the overlap interval of stability regions for the tangential and sagittal planes was maximal and equal to ~ 2.4 mm ($t_0 = 11.97 - 12.21$ cm). For the angle $\psi = 10^\circ$, the overlap interval of stability regions was ~ 0.6 mm ($t_0 = 12.06 - 12.12$ cm). The next calculation was performed for $\psi = 13.8^\circ$.

Our calculation also showed (Table 1) that the beam radii on the mirror R_1 in both planes decreased with increasing parameter t_0, whereas the beam radii on the mirror R_{11} had minima in the middle of the stability region (for $t_0 \sim 12.08$ cm). The values $t_0 = 11.98$ and 12.20 cm are located near the left and right boundaries of the stability region, respectively.

Table 1. Radii w_{1x}, w_{1y}, w_{11x}, w_{11y} of beams on mirrors R_1 and R_{11} and the waist radii w_x, and w_y in a crystal in the tangential and sagittal regions for different t_0.

t_0/cm	w_{1x}/mm	w_{1y}/mm	w_{11x}/mm	w_{11y}/mm	w_x/μm	w_y/μm
11.98	1.2	1.0	1.0	0.9	16.1	11.8
12.08	0.6	0.6	0.7	0.7	23.2	14.7
12.20	0.3	0.3	1.1	0.9	14.6	11.0

2.2 Beam focusing in a crystal

In calculations we compared cavity configurations with different radii of curvature R_1 and R_{11} of mirrors in the range of parameters t_0 and δt in which beam waists in both planes are located inside the crystal. For this purpose, we studied the position of beam waists in the crystal as a function of the distance t_3 and the crystal displacement δt (Fig. 1).

Note that beam waists in the x and y planes are separated in the crystal and have different values due to the cavity asymmetry and astigmatism. We found that variations of the parameters t_3 and δt could not provide the simultaneous position of beam waists at the crystal centre. Figure 2a presents the typical axial beam profile in the crystal for $t_0 = 12.08$ cm and $\delta t = 1.1$ mm, when the waists are located relatively symmetrically.

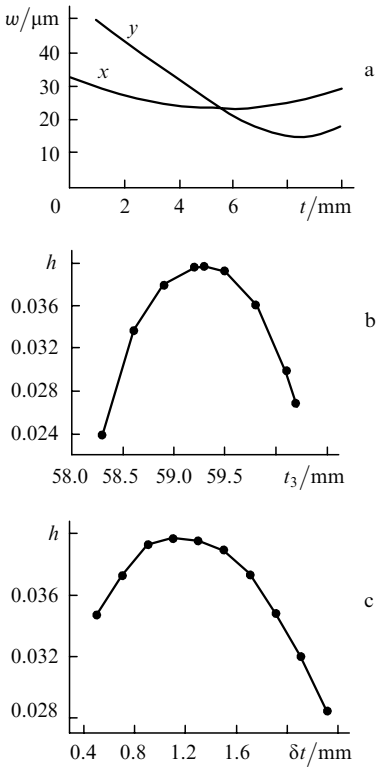

Figure 2. Axial dependences of the beam waists in the crystal in the x and y planes for $t_0 = 12.08$ cm and $\delta t = 1.1$ mm on t (a) and of the aperture function h on t_3 (b) and on the crystal displacement δt (c).

Such calculations were performed for all the six cavity configurations. Configuration 1 ($R_1 = 10$ m, $R_{11} = \infty$) was found to be optimal because it provides the best filling of the discharge tube upon optimal focusing of radiation into the crystal. In addition, it is more convenient to work with the plane mirror R_{11}.

2.3 Walk-off effect

The problem of second-harmonic generation in a focused beam requires the cavity optimisation taking into account the walk-off effect. In the case of weak focusing, the radiation intensity is low. In the case of tight focusing, the conversion efficiency is restricted due the beam divergence and the walk-off effect caused by the crystal anisotropy.

The second-harmonic power P_2 is usually written in the form [4]

$$P_2 = Klk_1 h(B, \Delta k, \xi_x, \xi_y, \mu_x, \mu_y) P_1^2 = \eta P_1^2, \quad (1)$$

where

$$K = \frac{2\mu_0^{3/2}\varepsilon_0^{1/2}\omega^2 d_{\text{eff}}^2}{\pi n_{\text{o1}}^2 n_{\text{e2}}}; \quad (2)$$

P_1 is the fundamental-wave power; l is the crystal length; k_1 is the wave vector of the fundamental harmonic inside the crystal; ε_0 and μ_0 are the dielectric constant and magnetic permeability, respectively; n_{o1} and n_{e2} are the refractive indices of the ordinary fundamental-harmonic wave and of the extraordinary second-harmonic wave, respectively; $d_{\text{eff}} = 1.34$ pm V^{-1} is the effective nonlinear coefficient of the BBO crystal (correspondingly, $K = 1.52 \times 10^{-8}$ W^{-1}); $h(B, \Delta k, \xi_x, \xi_y)$ is the aperture function, which for elliptic beams has the form (see, for example, [4])

$$h(B, \Delta k, \xi_x, \xi_y, \mu_x, \mu_y) = \frac{(\xi_x \xi_y)^{1/2}}{l^2}$$

$$\times \int_0^l \int_0^l \frac{\exp[\mathrm{i}\Delta k(z' - z)]\exp[-4B^2(z' - z)^2 \xi_y / l^2]\mathrm{d}z\mathrm{d}z'}{(1 + \mathrm{i}\tau_x')^{1/2}(1 + \mathrm{i}\tau_y')^{1/2}(1 - \mathrm{i}\tau_x)^{1/2}(1 - \mathrm{i}\tau_y)^{1/2}} \quad (3)$$

and has for each B the only maximum over ξ_x and ξ_y; $b_i = 2\pi n_{\text{o}} w_i^2/\lambda$; $\xi_i = l/b_i$; $\tau_i = 2(z - \mu_i)/b_i$; μ_i is the position of beam waists in the crystal (distance from the left crystal face) in the tangential and sagittal planes; and $\Delta\boldsymbol{k} = 2\boldsymbol{k}_1 - \boldsymbol{k}_2$. The dependence of the aperture function on the parameters B, ξ_x and ξ_y is considered in detail in [4]. The aperture function characterises the overlap of the fundamental and second-harmonic beams. The parameter $B = 0.5\rho(2\pi l n_0/\lambda)^{1/2} \approx 19.3$. The quantity $\eta = Klk_1 h$ is usually called the second-harmonic conversion coefficient. Due to the specific properties of our cavity, it is necessary to optimise the displacement of the crystal because the position of waists in the x and y planes is different.

We found the optimum of the aperture function over parameters t_3 and δt for which $t_3 = 5.93$ cm, $\delta t = 1.1$ mm (correspondingly, $t_0 = 12.08$ cm, $t_2 = 6.15$ cm). In the optimal case, the waists are located closer to the right face of the crystal; their position are $\mu_x = 5.4$ mm and $\mu_y = 8.4$ mm, the radii of waists are $w_x = 23.2$ μm and $w_y = 14.7$ μm. Figures 2b and c show the dependences of the aperture function h on parameters t_3 and δt near the optimum of the aperture function.

The optimal parameters $t_0 = 12.11$ cm and $\delta t = 1.2$ mm ($t_2 = 6.18$ cm and $t_3 = 5.94$ cm) obtained for the angle $\psi = 10^\circ$ weakly differ from the optimal parameters for $\psi = 13.8^\circ$: beam waists ($w_x = 21.8$ μm, $w_y = 10.1$ μm) are also located closer to the right face of the crystal ($\mu_x = 5.7$ mm, $\mu_y = 8,5$ mm). Note that the displacement of the waist with respect to the crystal centre in the tangential plane, where the walk-off is absent, is small.

As the parameters t_3 and δt were changed, the aperture integral h changed from 0.024 to 0.040. Thus, the calculated second-harmonic conversion coefficient η lies in the range $(7.82 - 13.07) \times 10^{-5}$ W^{-1}.

3. Experiment

Figure 3 shows the scheme of the experimental setup for measuring the fundamental radiation power P_1 ($\lambda = 488$ nm) and second-harmonic power P_2. Mirrors R_1, R_{11}, R_2, and R_3 and the crystal are fixed on flanges (denoted by dashed lines) connected by invar rods. The crystal is mounted inside a thermostat on a movable stage, which can be displaced along the beam direction and perpendicular to it, oriented at the Brewster angle and phase-matching angle, and rotated around the beam direction.

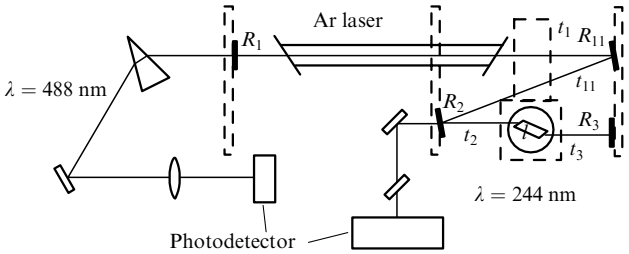

Figure 3. Scheme of the experimental setup.

The 488-nm line was selected by using selective mirrors. The cavity had the following parameters: mirrors $R_1 = 10$ m and $R_{11} = \infty$ had transmission $\sim 0.1\,\%$ at 488 nm; the transmission of mirrors $R_2 = 12.8$ cm and $R_3 = 6.0$ cm was $\sim 0.1\,\%$ at 488 nm and $\sim 80\,\%$ at 244 nm. The UV radiation power transmitted through mirrors R_2 and R_3 was measured.

We studied the dependences of the intracavity power of the fundamental and second harmonics on the displacement Δt_3 of the mirror R_3 and the displacement $\Delta\delta t$ of the crystal for the discharge tube current $J \simeq 100$ A. The dependences of P_1 and P_2 on the displacement Δt_3 of the mirror are presented in Fig. 4 [Δt_3 is the displacement of the mirror R_3 with respect to the optimal position for second harmonic generation (SHG)]. We found that for $\Delta t_3 > 0$, the higher transverse modes began to appear along with the TEM$_{00}$ mode. The integrated power P_1 increased, whereas the TEM$_{00}$ mode power decreased, resulting in the decrease of P_2. According to our calculations, the beam cross section

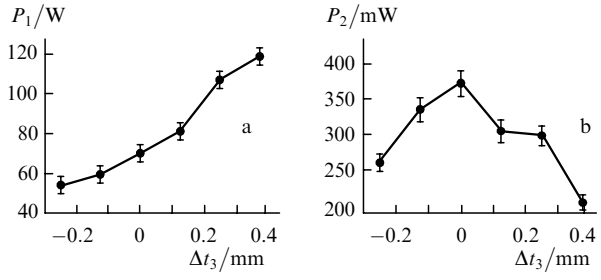

Figure 4. Dependences of the first- (a) and second-harmonic (b) powers on the displacement of the mirror R_3.

in the $R_1 - R_{11}$ arm decreases with increasing t_3. The TEM_{00} mode was selected by using an additional ~ 4-mm aperture.

Thus, the optimal power of the second harmonic obtained by varying t_3 is determined both by the optimum of the aperture integral and a change in the power of the fundamental harmonic. The stability region of the cavity in the experiment admitted the displacement of the mirror R_3 within ~ 2 mm, while the size of the stability region and the output UV power proved to be noncritical to the angle of incidence ψ on the mirror R_2: unlike the calculation, measurements at angles 12.3° and 10° gave close results.

In the next experiment, at the optimal position of the mirror R_3 ($\Delta t_3 = 0$), the crystal was displaced and the dependences of the powers of the first and second harmonics on $\Delta\delta t$ were measured (Fig. 5), where $\Delta\delta t$ is a change of the parameter δt with respect to the optimal position of the crystal at which the second-harmonic power is maximal. One can see from Fig. 5a that the first-harmonic power changes no more than by 10 %, whereas theoretically it should be constant over the entire range of δt. Its change in the experiment can be explained by the fact that the cavity was adjusted by the second-harmonic power. Therefore, the optimal power P_2 obtained upon crystal displacement is related only to the optimal value of the aperture integral. The final absolute values of optimal experimental parameters t_2 and t_3 for $\psi = 10^\circ$ were 5.9 and 6.0 cm, while the corresponding optimal theoretical parameters were 6.18 and 5.94, respectively (for the same angle).

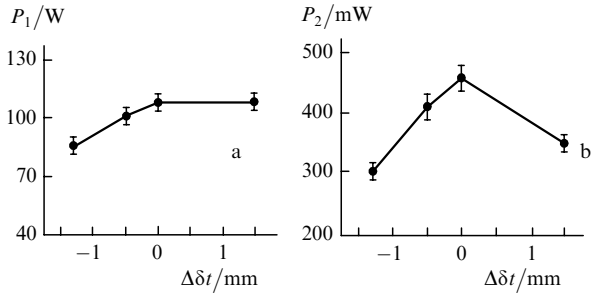

Figure 5. Dependences of the first- (a) and second-harmonic (b) powers on the displacement $\Delta\delta t$ of the crystal.

The difference between the theoretical and experimental values of the parameter t_2 can be explained by the fact that the crystal is strongly heated at radiation powers achieved in experiments (the temperature in the thermostat during SHG was $\sim 50\,^\circ$C), which results in the formation of a thermal lens, and to preserve optimal focusing at the right end of the crystal, the focusing mirror R_2 should be moved closer to the crystal; in this case, the position of the collimating mirror R_3 does not differ from the calculated position. The temperature phase-matching width is rather large, and this suggests that the discrepancy between the calculated and experimental data is determined by the thermal lens effect to a greater extent than by the violation of phase matching due to its finite temperature width. In addition, it follows from calculations that the smaller the sum $t_2 + t_3 = t_0$, the greater the beam cross section in the discharge tube. We will show below that an increase in the beam diameter in the discharge tube can noticeably change the optimal length of the focusing arm compared to its value corresponding to the optimum of the aperture integral.

The estimate of the intracavity first-harmonic power for the current $J = 125$ A gives $P_1 \simeq 108$ W, while the measured second-harmonic power is $P_2 \simeq 450$ mW. Taking into account that the total reflection and absorption losses on the mirror R_2 at 244 nm are ~ 25 % and Brewster losses on the crystal surface are ~ 20 %, we obtain that the real second-harmonic power P_2 generated in the travelling wave is ~ 750 mW, i.e., the conversion coefficient $\eta_{exp} \simeq 6.4 \times 10^{-5}$ W^{-1} is close to the calculated value, which lies in the range $(7.82 - 13.07) \times 10^{-5}$ W^{-1}.

In the additional experiment we measured the power of the 488-nm line of the laser. The output mirror had transmission 20 %, which was close to the optimal value for conditions when the second-harmonic power was measured as a function of the discharge current in the tube. Figure 6 shows the dependence of the optimal second-harmonic power on the maximum output power of the first harmonic, obtained for the same current.

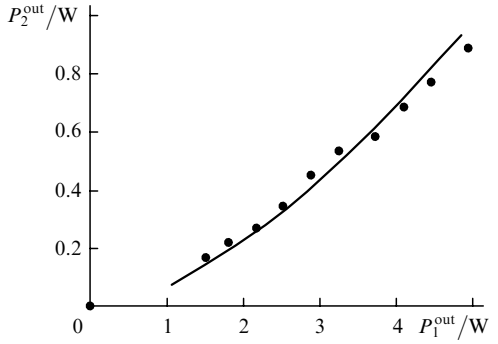

Figure 6. Dependence of the optimal second-harmonic power on the maximal first-harmonic power for the same parameters of the discharge (points are the experiment, the solid curve is the theory).

It is known that the gain saturation upon multimode oscillation in an argon ion laser is nearly homogeneous [11]. In the model of homogeneous saturation of the gain $g = g_0/(1 + 2I/I_s)$, the output radiation power at the fundamental frequency is described by the expression

$$P_1^{out} = \frac{T_1}{2} I_s \pi w^2 \left(\frac{g_0 2L}{\varkappa 2L + T_1} - 1 \right), \tag{4}$$

where I_s is the saturation intensity; g_0 is the gain; $w = 1.25$ mm is the beam radius; and $L = 1$ m is the active medium length. For the current $J = 125$ A, the saturation intensity is $I_s = I_s^{max} \approx 100$ W cm^{-2} (correspondingly, the saturation power is $P_s^{max} = I_s^{max} \pi w^2 \approx 4.9$ W), the gain for the same current is $g_0 = g_0^{max} \approx 1.4$ m^{-1}, $T_1 = 20$ % is the transmission coefficient of the output mirror, which is close to the optimal one when the adverse losses (not related to the SHG) are $\varkappa \approx 2.9$ % m^{-1}.

According to [12], the second-harmonic power for a sum of waves propagating in both directions in the model of homogeneous gain saturation is described by the approximate expression

$$P_2 = g_0 L I_s \pi w^2 f(s, t), \tag{5}$$

where

$$f(s,t)=\frac{1}{4s}\left\{\left[(t-s)^2+4s\right]^{1/2}-(t+s)\right\}^2. \quad (6)$$

Here,

$$t=\frac{\varkappa}{g_0}, \quad s=\frac{\eta I_s \pi w^2}{2g_0 L} \quad (7)$$

are the coefficients of linear and nonlinear losses, respectively. The estimated value of the coefficient of adverse losses in the crystal and the active element is $\sim 2.9\ \%\ \mathrm{m}^{-1}$ and the second-harmonic conversion coefficient is $\eta \approx 10^{-4}\ \mathrm{W}^{-1}$. For the current $J = 125$ A, the parameters t and s are $\sim 2.1\times10^{-2}$ and $\sim 1.8\times10^{-4}$, respectively.

The approximate theoretical dependence $P_2^{\mathrm{out}}(P_1^{\mathrm{out}})$ was constructed by using the experimental values of parameters P_s and g_0, which simultaneously varied with current approximately from $P_{\mathrm{s}}^{\max}/2$, $g_0^{\max}/2$ to $P_{\mathrm{s}}^{\max}$, $g_0^{\max}$. The theoretical dependence $P_2^{\mathrm{out}}(P_1^{\mathrm{out}})$ presented in Fig. 6 takes into account Brewster reflection losses on the crystal surface and reflection losses on cavity mirrors amounting to 40 %. One can see that the theory and experiment are in good agreement.

The function $f(s,t)$ achieves a maximum for $s = t$. In the case of low adverse losses ($t \ll 1$), the maximum of the function $f(t,t) \to 1$, and P_1^{out} and P_2 achieve the maximum $g_0 L I_{\mathrm{s}} \pi w^2$. In our case, nonlinear SHG losses are low ($s \ll t$). One can see from relations (7) that nonlinear losses can be increased by increasing the beam aperture w and the second-harmonic conversion coefficient η. It is known that in the case of a large walk-off ρ in a nonlinear crystal, the conversion efficiency η increases as $\sqrt{l}$ [13]. Thus, the ninefold increase in the crystal length will result in the threefold increase in the conversion efficiency η. Such crystals are expensive and their use will cause an increase in adverse losses in the cavity due to absorption of radiation in the crystal. On the other hand, the use of a wide-aperture discharge tube leads to the increase in nonlinear losses due to the increase in the active-medium area, thereby increasing the saturation power $P_{\mathrm{s}} \propto I_{\mathrm{s}} w^2$.

In the practically interesting case $1 \gg t \gg s$, the function $f(s,t)$ can be described by the approximate expression

$$f(s,t)\approx 1+2\frac{t^2}{4s}\left[1-\left(1+\frac{4s}{t^2}\right)^{1/2}\right]. \quad (8)$$

For two limiting cases, we have

$$f(s,t)\approx\begin{cases} s/t^2 & \text{for } 4s \ll t^2,\\ 1-t/\sqrt{s} & \text{for } 4s \gg t^2.\end{cases} \quad (9)$$

One can see that the second-harmonic power is an exponential function of the beam size in a discharge tube: $P_2 \propto \eta I_s^2 w^4$ for low nonlinear losses; as ηP_s increases, the function $f(s,t) \to 1$ and the power $P_2 \to P_{\mathrm{s}} g_0 L$, which corresponds to the 100 % conversion. Here, we analyse an intermediate case: $t^2 \approx 4\times10^{-4}$, $4s \approx 7\times10^{-4}$; in this case, the function $f(s,t) \approx 0.25$. The function $f(s,t)$ also increases with increasing the beam cross section in the discharge tube, which determines to a great extent the increase in the conversion coefficient compared to that for capillary tubes. The maximum first-harmonic power at 488 nm with the output mirror having transmission 20 % is ~ 5 W, while the total second-harmonic power generated in the crystal, taking losses into account, is ~ 1.5 W. Therefore, the conditional conversion efficiency is $\sim 30\ \%$.

4. Conclusions

By using intracavity frequency doubling in an argon laser, we have obtained the second-harmonic power $P_2 \gtrsim 1$ W at 244 nm, which is twice as large as that for known analogues. This increase was achieved by increasing the aperture of the fundamental beam in the discharge tube. The second-harmonic conversion coefficient is close to its calculated value. Optimisation was performed by adjusting the focusing $R_2 - R_3$ arm of the cavity and the position of a crystal in it.

We have shown that the dependence of the optimal second-harmonic power on the displacement of the crystal position with respect to the focal point is related to the optimum of the aperture integral. The optimum depending on the focusing arm length is determined to a greater extent not by the optimum of the aperture integral but by a change in the fundamental radiation power due to a change in the beam size in the active medium (discharge tube) and the corresponding change in the saturation conditions in the active medium.

We have shown that the second-harmonic power can be further increased by increasing the fundamental radiation power (no saturation was observed in experiments).

Acknowledgements. This work was supported by a program of the Russian Academy of Sciences and the program of Support of the Leading Scientific Schools. The authors thank M.A. Rybakov for his technical assistance.

References

1. Kashayap R. *Fiber Bragg Gratings* (New York: Acad. Press, 1999).
2. Dowley M.W. *Appl. Phys. Lett.*, **13**, 395 (1968).
3. Taira Y. *Jpn. J. Appl. Phys.*, **31**, L682 (1992).
4. Steinbach A., Rauner M., Cruz F.C., Bergquist J.C. *Opt. Commun.*, **123**, 207 (1996).
5. Hansch T.W., Couillaud B. *Opt. Commun.*, **35**, 441 (1980).
6. Berkeland D.J., Cruz F.C., Bergquist J.C. *Appl. Opt.*, **36**, 4159 (1997).
7. Svalgaard M., Gilbert S.L. *Appl. Opt.*, **36**, 4999 (1997).
8. Alferov G.N., Grigor'ev V.A., Donon V.I. *Kvantovaya Elektron.*, **5**, 29 (1978) [*Sov. J. Quantum Electron.*, **8**, 12 (1978)].
9. Kato K. *IEEE J. Quantum Electron.*, **22**, 1013 (1986).
10. Prokhorov A.M. (Ed.) *Spravochnik po lazeram* (Handbook on Lasers) (Moscow: Sov. Radio, 1978) Vol. 2.
11. Davis C.C., King T.A., in *Advances in Quantum Electronics*. Ed. by D.W. Goodwin (New York: Acad. Press, 1975) Vol. 3, p. 169.
12. Dmitriev V.G., Tarasov L.V. *Prikladnaya nelineinaya optika* (Applied Nonlinear Optics) (Moscow: Radio i Svyaz', 1982).
13. Boyd G.D., Kleinman D.A. *J. Appl. Phys.* **39**, 3597 (1968).